Bulletin of the Institute of Mathematics
Academia Sinica (New Series)
Vol. **15** (2020), No. 3, pp. 187-216
DOI: 10.21915/BIMAS.2020301

N-WAVES FOR CONSERVATION LAWS WITH LINEAR DEGENERACY

TAI-PING LIU

Institute of Mathematics, Academia Sinica, Taipei.
Department of Mathematics, Stanford University, USA.
E-mail: tpliu@math.sinica.edu.tw

Abstract

For system of hyperbolic conservation laws with genuinely nonlinear characteristic fields, it has been shown that a solution with compact supported perturbation of constant state tends to the superposition of N-waves, with two time invariants for each characteristic field. The aim of the present article is to generalize the result to systems with both genuinely nonlinear and linearly degenerate characteristic fields, so that the result applies to the Euler equations in gas dynamics, magnetohydrodynamics equations, and full nonlinear elasticity equations.

1. Introduction

Consider system of hyperbolic conservation laws

$$\boldsymbol{u}_t + \boldsymbol{f}(\boldsymbol{u})_x = \boldsymbol{0},\ \boldsymbol{u} \in \mathbb{R}^n. \tag{1.1}$$

The system is assumed to be strictly hyperbolic, with the eigenvectors normalized:

$$\begin{aligned}\boldsymbol{f}'(\boldsymbol{u})\boldsymbol{r}_i(\boldsymbol{u}) = \lambda_i(\boldsymbol{u})\boldsymbol{r}_i(\boldsymbol{u}),\ \boldsymbol{l}_i(\boldsymbol{u})\boldsymbol{f}'(\boldsymbol{u}) = \lambda_i(\boldsymbol{u})\boldsymbol{l}_i(\boldsymbol{u}),\\ \boldsymbol{l}_i(\boldsymbol{u})\boldsymbol{r}_j(\boldsymbol{u}) = \delta_{ij},\ i,j = 1,2,\dots,n,\\ \lambda_1(\boldsymbol{u}) < \lambda_2(\boldsymbol{u}) < \cdots < \lambda_n(\boldsymbol{u}).\end{aligned} \tag{1.2}$$

Received September 10, 2020 and in revised form October 19, 2020.

AMS Subject Classification: 35L65, 76J20.

Key words and phrases: Hyperbolic conservation laws, shock waves, N-waves.

The research is supported by MOST Grant 106-2115-M-001-011-, Simons Foundation Grant and Institute of Mathematics, Academia Sinica.

Each i-characteristic field is either genuinely nonlinear in that the i-th characteristic value λ_i is strictly monotone in its characteristic direction $\boldsymbol{r}_i$, [7]:

$$\nabla\lambda_i(\boldsymbol{u})\cdot\boldsymbol{r}_i(\boldsymbol{u})\neq 0,\ \text{for } i\in I, \text{ genuinely nonlinear;} \tag{1.3}$$

or linearly degenerate in that the i-th characteristic value λ_i is constant in its characteristic direction $\boldsymbol{r}_i$:

$$\nabla\lambda_i(\boldsymbol{u})\cdot\boldsymbol{r}_i(\boldsymbol{u})=0,\quad \text{for } i\in II, \text{ linearly degenerate,} \tag{1.4}$$

for all states $\boldsymbol{u}$ under consideration. We have $I\cup II=\{1,2,\dots,n\}$.

Our aim is to study the time-asymptotic shape of the solution when the initial datum is a compactly supported perturbation of a constant state $\boldsymbol{u}_0$:

$$\begin{aligned}&\boldsymbol{u}_t+\boldsymbol{f}(\boldsymbol{u})_x=0,\\ &\boldsymbol{u}(x,0)=\boldsymbol{u}_0 \text{ for } |x|>M,\ TV\equiv var(\boldsymbol{u}(\cdot,0)) \text{ small.}\end{aligned} \tag{1.5}$$

For the inviscid Burgers equation $u_t+(u^2/2)_x=0$, such a solution tends to the centered N-waves $u(x,t)=N_{p,q}(x,t)$, each depending on two parameters $p\leq 0\leq q$, Figure 1:

$$N_{p,q}(x,t)=\begin{cases}0, & x<-\sqrt{-2pt},\\ \frac{x}{t}, & -\sqrt{-2pt}<x<\sqrt{2qt},\\ 0, & x>\sqrt{2qt}.\end{cases} \tag{1.6}$$

Here, for simplicity, we have taken the base state $u_0=0$. The N-wave consists of centered rarefaction wave sandwiched by the shock waves at $x=-\sqrt{-2pt}$ on the left and at $x=\sqrt{2qt}$ on the right. The two time invariants p and q, $p\leq 0\leq q$, are determined from the initial data

$$\begin{aligned}&p=\min_x\int_{-\infty}^x u(y,0)dy=\min_x\int_{-\infty}^x u(y,t)dy,\\ &q=\max_x\int_x^{\infty} u(y,0)dy=\max_x\int_x^{\infty} u(y,t)dy,\ t\geq 0.\end{aligned} \tag{1.7}$$

The corresponding notion of N-waves can be defined approximately as simple waves pertaining to a genuinely nonlinear i-characteristic field, $i\in I$

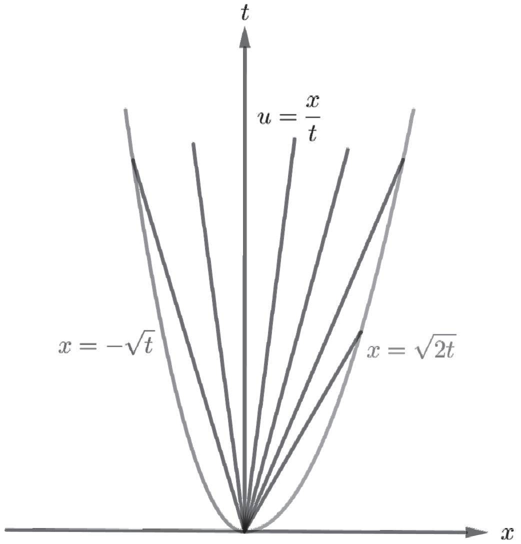

Figure 1: N-wave $N_{-1/2,1}$.

as follows. Consider the i-th characteristic curve $\boldsymbol{R}_i(\boldsymbol{u}_0)$, which is the integral curve of $\boldsymbol{r}_i(\boldsymbol{u})$ through a given state $\boldsymbol{u}_0$. It is easily shown that for $\boldsymbol{u}(x,t) \in \boldsymbol{R}_i(\boldsymbol{u}_0)$ to be a smooth solution of the system (1.1), its characteristic speed $\lambda_i(\boldsymbol{u})$ must satisfies the inviscid Burgers equation, see Section 2. Thus the i-th N-wave $\boldsymbol{N}_{p_i,q_i}(x,t) = \boldsymbol{N}_{p_i,q_i}(\boldsymbol{u}_0)(x,t)$ for the system through a state $\boldsymbol{u}_0$ with parameters p_i and $q_i,\ p_i \le 0 \le q_i$ is defined by its characteristic speed $\lambda_i(\boldsymbol{u})$, Figure 2:

$$\begin{aligned} &\lambda_i(\boldsymbol{N}_{p_i,q_i})(x,t) \equiv \begin{cases} \lambda_i(\boldsymbol{u}_0),\ x - \lambda_i(\boldsymbol{u}_0)t < -\sqrt{-2pt}, \\ \frac{x}{t},\ -\sqrt{-2pt} < x < \sqrt{2qt}, \\ \lambda_i(\boldsymbol{u}_0),\ x - \lambda_i(\boldsymbol{u}_0)t > \sqrt{2qt}; \end{cases} \\ &\boldsymbol{N}_{p_i,q_i}(x,t) \in \boldsymbol{R}_i(\boldsymbol{u}_0). \end{aligned} \tag{1.8}$$

Divide the (x,t) space into regions

$$\begin{aligned} \tilde{\Omega}_1 \equiv \{(x,t):\ x < \tilde{\lambda}_1 t\},\ \tilde{\Omega}_n \equiv \{(x,t):\ x > \tilde{\lambda}_{n-1} t\}, \\ \tilde{\Omega}_i \equiv \{(x,t):\ \tilde{\lambda}_{i-1} t < x < \tilde{\lambda}_i t\},\ i = 2, \dots, n-1, \end{aligned} \tag{1.9}$$

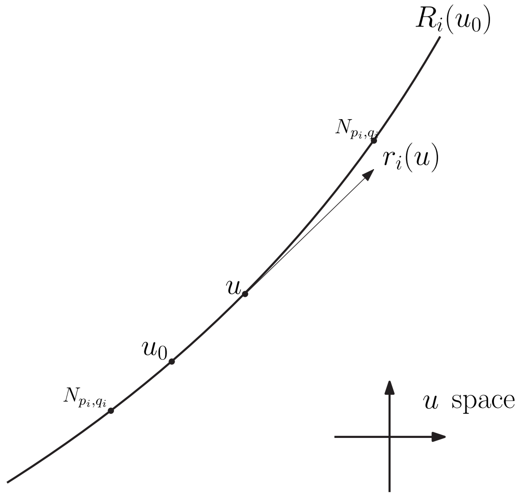

Figure 2: N-wave for i-th characteristic field.

where $\tilde{\lambda}_i,\ i = 1, \ldots, n-1$ are constants chosen such that $\lambda_i(\boldsymbol{u}) < \tilde{\lambda}_i < \lambda_{i+1}(\boldsymbol{u})$ for all states $\boldsymbol{u}$ under consideration. The i-th N-wave $\boldsymbol{N}_{p_i,q_i}(x,t)$ is an exact solution to the system (1.1) except for the two shock waves. Nevertheless, we will see that it is an accurate time-asymptotic state.

Theorem 1.1. *Suppose the total variation TV of the initial data is sufficiently small. Then the initial value problem* (1.5) *has a solution global in time and tends to the superposition of N-waves and linear waves in the following sense:*

(1) *For each $i \in I$, there exist two time invariants p_i and q_i, such that the solution $\boldsymbol{u}(x,t),\ (x,t) \in \tilde{\Omega}_i$, tends to N-wave $\boldsymbol{N}_{p_i,q_i}(x,t)$ as $t \to \infty$.*

(2) *For each $i \in II$, the solution $\boldsymbol{u}(x,t),\ (x,t) \in \tilde{\Omega}_i$, tends to a linear wave with speed $\lambda_i(\boldsymbol{u}_0)$ and taking values on $\boldsymbol{R}_i(\boldsymbol{u}_0)$ as $t \to \infty$.*

(3) *The time-asymptotic convergence rate in the $L_1(x)$ norm to linear waves is $t^{-1/2}$ and to N-waves is $t^{-1/4}$.*

The study of N-waves for scalar laws was initiated in Friedrichs [3] in the study of flow pattern around a supersonic airfoil, and subsequently by Hopf [6], through the inviscid limit of Burgers equation. For two conservation laws, $n = 2$, there exists a coordinates of Riemann invariants and the wave coupling measured in that coordinates is third order. Decay of solutions to the genuinely nonlinear two conservation laws was shown in an unpublished note related to Glimm-Lax [5]. This allows for the generalization of the N-wave theory for scalar laws to the 2×2 genuinely nonlinear systems by DiPerna[1]. In [9], it was recognized that, the characteristic speed λ_i for the i-th simple waves satisfies the inviscid Burgers equation and the third order coupling can be attained for general genuinely nonlinear systems, $n \geq 2$. Decay and convergence to N-waves are also shown for genuinely nonlinear systems in [9]. The optimal convergence rate is attained in [12] after some pointwise analysis. In the present article, the system is allowed to have linearly degenerate fields, and third order coupling in terms of the decaying modes does not hold in finite time. Waves pertaining to linear degenerate fields interact among themselves and with waves pertaining to genuinely nonlinear fields, as in the case of magnetohydrodynamics, [10]. Because waves pertaining to linear degenerate fields do not decay, third order coupling in terms of the decaying modes does not hold. A careful analysis of repeated wave couplings is applied in place of the third order coupling used perviously. In Section 1, we briefly review the notion of simple waves in order to understand the time asymptotic states $\boldsymbol{N}_{p,q}$, (1.8). Our analysis is based on the existence theory of Glimm [4] through the wave tracing technique of [8], which is reviewed in Section 3. In Section 4, we carry out the analysis of wave coupling aforementioned, see also Remark 5.3 there. In Section 5, we study the decay of solutions, combining the decay analysis of the unpublished note related to Glimm-Lax [5] and the wave coupling analysis in Section 4. The convergence to N-waves is shown in Section 6, using the coupling estimate in Section 5 and generalizing the analysis in [1], [9] and [12]. Finally the convergence to linear waves is shown in Section 7.

2. Simple Waves

An i-th simple wave takes values along an i-th characteristic curve $\boldsymbol{R}_i(\boldsymbol{u}_0)$, Figure 2. Parametrize the curve by a non-singular parameter τ so that, for some positive scalar factor $\alpha(\boldsymbol{u})$,

$$\frac{d\boldsymbol{u}}{d\tau} = \alpha(\boldsymbol{u})\boldsymbol{r}_i(\boldsymbol{u}),\ \ \boldsymbol{u} \in \boldsymbol{R}_i(\boldsymbol{u}_0),\ \ i - \text{characteritstic curve}. \tag{2.1}$$

By the chain rule,

$$\begin{aligned}\frac{\partial}{\partial x}\boldsymbol{u}(x,t) &= \frac{\partial \tau}{\partial x}\frac{d\boldsymbol{u}}{d\tau} = \big(\frac{\partial \tau}{\partial x}\alpha(\boldsymbol{u})\big)\boldsymbol{r}_i(\boldsymbol{u}(x,t)),\\ \frac{\partial}{\partial t}\boldsymbol{u}(x,t) &= \frac{\partial \tau}{\partial t}\frac{d\boldsymbol{u}}{d\tau} = \big(\frac{\partial \tau}{\partial t}\alpha(\boldsymbol{u})\big)\boldsymbol{r}_i(\boldsymbol{u}(x,t)),\\ \boldsymbol{u}_t + \boldsymbol{f}(\boldsymbol{u})_x &= \Big(\frac{\partial \tau}{\partial t} + \lambda_i\frac{\partial \tau}{\partial x}\alpha(\boldsymbol{u})\Big)\boldsymbol{r}_i(\boldsymbol{u}(x,t)).\end{aligned} \tag{2.2}$$

Thus for $\boldsymbol{u}(x,t)$ to be a solution of the conservation laws $\boldsymbol{u}_t + \boldsymbol{f}(\boldsymbol{u})_x = \boldsymbol{0}$, we need to require $\tau(\boldsymbol{u}(x,t))$ to satisfy, as $\boldsymbol{u}$ moves along $\boldsymbol{R}_i(\boldsymbol{u}_0)$,

$$\frac{\partial}{\partial t}\tau(\boldsymbol{u}) + \lambda_i(\boldsymbol{u})\frac{\partial}{\partial x}\tau(\boldsymbol{u}) = 0. \tag{2.3}$$

When the i-th characteristic field is genuinely nonlinear, (1.3), we may take the parameter $\tau = \lambda_i(\boldsymbol{u})$ and normalize the right eigenvector $\boldsymbol{r}_i(\boldsymbol{u})$ so that

$$\nabla\lambda_i(\boldsymbol{u})\cdot\boldsymbol{r}_i(\boldsymbol{u}) = 1. \tag{2.4}$$

Equation (2.3) becomes the inviscid Burgers equation

$$\lambda_t + \lambda\lambda_x = 0,\ \lambda \equiv \lambda_i(\boldsymbol{u}). \tag{2.5}$$

The above procedure yields an explicit way of constructing i-simple waves by first taking the initial values to satisfy $\boldsymbol{u}(x,0)\in\boldsymbol{R}_i(\boldsymbol{u}_0)$ and then set

$$\lambda_i(\boldsymbol{u}(x,0)) \equiv \lambda(x,0),\ \lambda_t + \lambda\lambda_x = 0,\ \lambda_i(\boldsymbol{u})(x,t) \equiv \lambda(x,t),\ \boldsymbol{u}(x,t)\in\boldsymbol{R}_i(\boldsymbol{u}_0). \tag{2.6}$$

The inviscid Burgers equation has the centered rarefaction wave solution connecting two states λ_0 and λ_1 with $\lambda_0 < \lambda_1$:

$$\lambda(x,t) = \begin{cases}\lambda_0, \text{ for } x < \lambda_0 t,\\ \frac{x}{t}, \text{ for } \lambda_0 t < x < \lambda_1 t,\\ \lambda_1, \text{ for } x > \lambda_1 t.\end{cases} \tag{2.7}$$

From (2.6) and (2.7), we can construct the i-th centered rarefaction waves

$(\boldsymbol{u}_0, \boldsymbol{u}_1)$ for the system (1.1):

$$\begin{aligned}\lambda_i(\boldsymbol{u})(x,t) \equiv &\begin{cases}\lambda_i(\boldsymbol{u}_0), \ x < \lambda_i(\boldsymbol{u}_0)t,\\ \frac{x}{t}, \ \lambda_i(\boldsymbol{u}_0)t < x < \lambda_i(\boldsymbol{u}_1)t,\\ \lambda_i(\boldsymbol{u}_1), \ x > \lambda_i(\boldsymbol{u}_1)t;\end{cases}\\ \boldsymbol{u}_1, \ \boldsymbol{u}(x,t) \in &\boldsymbol{R}_i(\boldsymbol{u}_0), \ \lambda_i(\boldsymbol{u}_0) < \lambda_i(\boldsymbol{u}_1).\end{aligned} \tag{2.8}$$

The above analysis applies only for smooth solutions of the inviscid Burgers equation and explains the rarefaction waves between the two shocks in the N-wave $\boldsymbol{N}_{p_i,q_i}(x,t)$ in (1.8). The analysis of the two shocks in $\boldsymbol{N}_{p_i,q_i}(x,t)$ will be done in the next section on the general consideration of shock waves. The construction in (2.8) yields solutions global in time; but that of (2.6) may form compression waves at later time and the construction fails.

For linear degenerate i-th field, there is a construction of global in time simple waves along an i-characteristic curve by free transporting along the characteristic $dx/dt = \lambda_i(\boldsymbol{u}_0) = \lambda_i(\boldsymbol{u}(x,0)), \ -\infty < x < \infty$:

$$\boldsymbol{u}(x,t) \equiv \boldsymbol{u}(x - \lambda_i(\boldsymbol{u}_0)t, 0), \ \boldsymbol{u}(x,0) \in \boldsymbol{R}_i(\boldsymbol{u}_0). \tag{2.9}$$

3. Riemann Problem

A jump discontinuity $(\boldsymbol{u}_-, \boldsymbol{u}_+)$ with speed s for the system (1.1) satisfies

$$s(\boldsymbol{u}_+ - \boldsymbol{u}_-) = \boldsymbol{f}(\boldsymbol{u}_+) - \boldsymbol{f}(\boldsymbol{u}_-), \ \text{Rankine-Hugoniot condition.} \tag{3.1}$$

It says that the two states are connected by a Hugoniot curve, $\boldsymbol{u}_+ \in \boldsymbol{H}(\boldsymbol{u}_-)$.

Definition 3.1. For a given state $\boldsymbol{u}_0$, the Hugoniot set $\boldsymbol{H}(\boldsymbol{u}_0)$ consists of all states $\boldsymbol{u}$ with the property that the two vectors $\boldsymbol{u} - \boldsymbol{u}_0$ and $\boldsymbol{f}(\boldsymbol{u}) - \boldsymbol{f}(\boldsymbol{u}_0)$ are parallel:

$$\begin{aligned}\boldsymbol{H}(\boldsymbol{u}_0) \equiv \{\boldsymbol{u} : \ &\sigma(\boldsymbol{u} - \boldsymbol{u}_0) = \boldsymbol{f}(\boldsymbol{u}) - \boldsymbol{f}(\boldsymbol{u}_0),\\ &\text{for some scalar } \sigma = \sigma(\boldsymbol{u}_0, \boldsymbol{u})\}, \ \text{Hugoniot set.}\end{aligned} \tag{3.2}$$

The following theorem is proved by the implicit function theorem, [7].

Theorem 3.2. *In a small neighborhood around a given state* $\boldsymbol{u}_0$ *the Hugoniot set* $\boldsymbol{H}(\boldsymbol{u}_0)$ *consists of* n *Hugoniot curves* $\boldsymbol{H}_j(\boldsymbol{u}_0)$, $j = 1, 2, \ldots, n$, *with the following properties:*

(i) $\boldsymbol{H}_j(\boldsymbol{u}_0)$ *is tangent to the characteristic curve* $\boldsymbol{R}_j(\boldsymbol{u}_0)$ *at* $\boldsymbol{u} = \boldsymbol{u}_0$ *and the shock speed* $\sigma(\boldsymbol{u}, \boldsymbol{u}_0)$ *tends to* $\lambda_j(\boldsymbol{u}_0)$ *as* $\boldsymbol{u}$ *approaches* $\boldsymbol{u}_0$ *along* $\boldsymbol{H}_j(\boldsymbol{u}_0)$.

(ii) *The characteristic curve* $\boldsymbol{R}_j(\boldsymbol{u}_0)$ *and the Hugoniot curve* $\boldsymbol{H}_j(\boldsymbol{u}_0)$ *have second order tangency at* $\boldsymbol{u} = \boldsymbol{u}_0$. *For a given state* $\boldsymbol{u}$ *on* $\boldsymbol{H}_j(\boldsymbol{u}_0)$, *there exists another state* $\bar{\boldsymbol{u}}$ *on* $\boldsymbol{R}_j(\boldsymbol{u}_0)$ *such that* $|\boldsymbol{u} - \bar{\boldsymbol{u}}| = O(1)|\boldsymbol{u} - \boldsymbol{u}_0|^3$, *Figure 3.*

(iii) *The shock speed is approximated by the arithmetic mean of the characteristic speed of its end states:*

$$\sigma(\boldsymbol{u}, \boldsymbol{u}_0) = \frac{\lambda_j(\boldsymbol{u}) + \lambda_j(\boldsymbol{u}_0)}{2} + O(1)|\boldsymbol{u} - \boldsymbol{u}_0|^2, \ \boldsymbol{u} \in \boldsymbol{H}_j(\boldsymbol{u}_0). \tag{3.3}$$

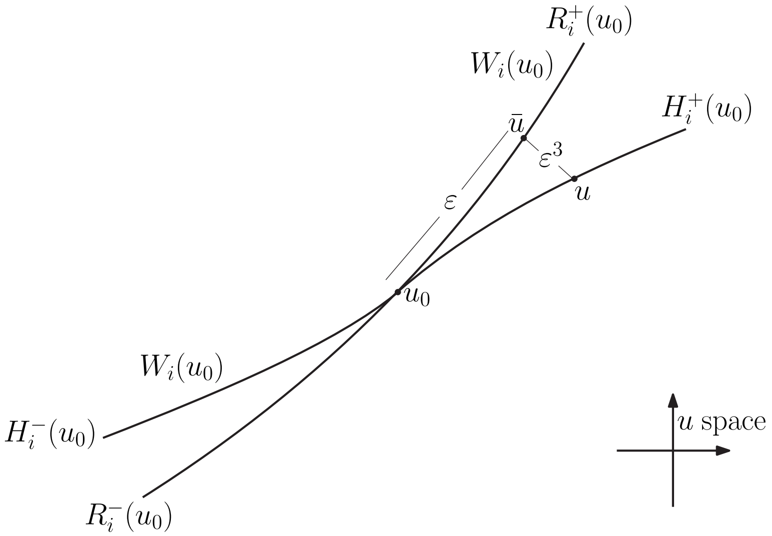

Figure 3: Wave curve for genuinely nonlinear field.

From Theorem 3.2, the two shock waves in the N-wave $\boldsymbol{N}_{p_i,q_i}(x,t)$ violates the Rankine-Hugoniot condition by an amount of $O(1)t^{-3/2}$ as $t \to \infty$. We will see that this is of sufficient accuracy for our time-asymptotic analysis.

For a genuinely nonlinear i-field, the i-characteristic curve $\boldsymbol{R}_i(\boldsymbol{u}_0)$ and i-th Hugoniot curve $\boldsymbol{H}_i(\boldsymbol{u}_0)$ are divided according to the parameter λ_i:

$$\begin{aligned}&\boldsymbol{R}_i(\boldsymbol{u}_0) = \boldsymbol{R}_i^+(\boldsymbol{u}_0) \cup \boldsymbol{R}_i^-(\boldsymbol{u}_0),\\ &\quad \lambda_i(\boldsymbol{u}) > \lambda_i(\boldsymbol{u}_0),\ \text{for } \boldsymbol{u} \in \boldsymbol{R}_i^+(\boldsymbol{u}_0);\ \lambda_i(\boldsymbol{u}) \leq \lambda_i(\boldsymbol{u}_0),\ \text{for } \boldsymbol{u} \in \boldsymbol{R}_i^-(\boldsymbol{u}_0),\\ &\boldsymbol{H}_i(\boldsymbol{u}_0) - \{\boldsymbol{u}_0\} = \boldsymbol{H}_i^+(\boldsymbol{u}_0) \cup \boldsymbol{H}_i^-(\boldsymbol{u}_0),\\ &\quad \lambda_i(\boldsymbol{u}) > \sigma(\boldsymbol{u}_0, \boldsymbol{u}) > \lambda_i(\boldsymbol{u}_0),\ \text{for } \boldsymbol{u} \in \boldsymbol{H}_i^+(\boldsymbol{u}_0);\\ &\quad \lambda_i(\boldsymbol{u}) < \sigma(\boldsymbol{u}_0, \boldsymbol{u}) < \lambda_i(\boldsymbol{u}_0),\ \text{for } \boldsymbol{u} \in \boldsymbol{H}_i^-(\boldsymbol{u}_0).\end{aligned} \tag{3.4}$$

Definition 3.3. Suppose that the i-characteristic field is genuinely nonlinear. An i-shock wave $\boldsymbol{u}_+ \in \boldsymbol{H}_i(\boldsymbol{u}_-)$, is admissible if it satisfies

$$\begin{cases}\lambda_i(\boldsymbol{u}_+) < \sigma(\boldsymbol{u}_-, \boldsymbol{u}_+) < \lambda_i(\boldsymbol{u}_-),\\ \lambda_j(\boldsymbol{u}) < \sigma(\boldsymbol{u}_-, \boldsymbol{u}_+),\ \text{for } j < i,\\ \sigma(\boldsymbol{u}_0, \boldsymbol{u}) < \lambda_j(\boldsymbol{u}_0),\ \text{for } i < j.\end{cases} \qquad \text{Lax entropy condition.} \tag{3.5}$$

By (3.3) and strict hyperbolicity, Lax entropy condition holds locally for half of the Hugoniot curve:

$$\lambda_i(\boldsymbol{u}_+) < \sigma(\boldsymbol{u}_-, \boldsymbol{u}_+) < \lambda_i(\boldsymbol{u}_-),\ \text{for } \boldsymbol{u}_+ \in \boldsymbol{H}_i^-(\boldsymbol{u}_-).$$

For the construction of rarefaction wave $(\boldsymbol{u}_0, \boldsymbol{u}_1)$ in (2.8), we need $\boldsymbol{u}_1 \in \boldsymbol{R}_i^+(\boldsymbol{u}_0)$. When the i-characteristic field is genuinely nonlinear, a state $\boldsymbol{u}_1$ is on the wave curve $\boldsymbol{W}(\boldsymbol{u}_0)$ form either a shock or rarefaction wave $(\boldsymbol{u}_0, \boldsymbol{u}_1)$, Figure 3:

$$\boldsymbol{W}_i(\boldsymbol{u}_0) \equiv \boldsymbol{R}_i^+(\boldsymbol{u}_0) \cup \boldsymbol{H}_i^-(\boldsymbol{u}_0),\quad \text{wave curve for genuinely nonlinear } i\text{-field.} \tag{3.6}$$

For linearly degenerate field, the wave curve is identical to the characteristic curve, $\boldsymbol{W}_i(\boldsymbol{u}_0) \equiv \boldsymbol{R}_i(\boldsymbol{u}_0)$ and linear waves with speed $\lambda_i(\boldsymbol{u}_0)$ can be constructed to take values on $\boldsymbol{R}_i(\boldsymbol{u}_0)$, (2.9).

The Riemann problem

$$\boldsymbol{u}_t + \boldsymbol{f}(\boldsymbol{u})_x = 0,\ \boldsymbol{u}(x,0) = \begin{cases}\boldsymbol{u}_l,\ x < 0,\\ \boldsymbol{u}_r,\ x > 0,\end{cases} \tag{3.7}$$

is solved by i waves $(\boldsymbol{u}_{i-1}, \boldsymbol{u}_i),\ i = 1, \ldots, n$, satisfying

$$\boldsymbol{u}_0 = \boldsymbol{u}_l,\ \boldsymbol{u}_n = \boldsymbol{u}_r,\ \boldsymbol{u}_i \in \boldsymbol{W}_i(\boldsymbol{u}_{i-1}),\ i = 1, 2, \ldots, n. \tag{3.8}$$

The existence of these states follows from the implicit function theorem using Theorem 3.2.

4. Glimm Estimates

The Glimm scheme constructs the approximate solutions using the solutions of Riemann problem as building blocks. The Glimm functional $F(t)$ measures the potential of wave interactions after time t. It consists of several components. The total amount of waves at time t is denoted by the linear term $L(t)$. There is the quadratic $Q_d^{ij}(t)$ denoting the potential of interaction of waves of the i-th characteristic family and waves of the j-th characteristic family, $i \neq j$. A third order term $Q_s^i(t)$ denotes the potential of interaction of waves of the genuinely nonlinear i-th characteristic family, $i \in I$. The functional is defined for a space-like curve J:

$$\begin{aligned}
L(J) &\equiv \sum\{\alpha:\ \alpha \text{ strength of waves crossing } J\};\\
Q_d^{ij}(J) &\equiv \{\alpha_i\beta_j:\ \alpha_i \text{ strength of } i\text{-wave to the left, } \beta_j \text{ strength of } j\\
&\qquad \text{waves to the right crossing } J,\ i > j,\ i,j = 1, \ldots, n\};\\
Q_s^i(J) &\equiv \{\alpha\beta(\alpha+\beta):\ \alpha, \beta\ i\text{-waves crossing } J \text{ and}\\
&\qquad\qquad \text{at least one of them a shock}\};\\
Q_d(J) &\equiv \sum_{i>j} Q_d^{ij}(J),\\
Q_s(t) &\equiv \sum_{i\in I} Q_s^i(J);\ F(J) \equiv L(J) + AQ_d(J) + AQ_s(J).
\end{aligned} \tag{4.1}$$

By analysis of local wave interaction, it is shown that the functional $F(J)$ decreases as the space-like curve pushes in forward time direction. Let J be the curve around time t, then the above functionals are denoted by $L(t),\ Q_s(t), Q_d(t)$, etc. Given a region Ω in the (x,t) space. Set

$$\begin{aligned}
&D_d(\Omega),\ D_s(\Omega),\ D(\Omega) \equiv D_d(\Omega) + D_s(\Omega):\\
&\qquad \text{the amount of wave interaction occurs in } \Omega.
\end{aligned} \tag{4.2}$$

For $\Omega = \{(x,t) : \ t > t_0\}$, write $D_d(\Omega) = D_d(t_0),\ D_s(\Omega) = D_s(t_0)$. The Glimm's estimate yields

$$D(t) = O(1)\big(Q_d(t) + Q_s(t)\big). \tag{4.3}$$

Thus we often use $Q_d(t),\ Q_s(t)$ when $D_d(t),\ D_s(t)$ can be used for more accurate estimate, e.g., (5.6).

5. Coupling of Waves

The solutions for system of hyperbolic conservation laws are constructed by the Glimm scheme, [4], when the total variation TV, (1.5), of the initial data is small. It is shown by using the Glimm functional that the total variation of the solution $\boldsymbol{u}(\cdot,t)$ at any time $t \geq 0$ is $O(1)TV$. The i-waves pertaining to the genuinely nonlinear fields, $i \in I$, decay; while the i-waves pertaining to linearly degenerate fields $i \in II$ behave like linear waves and do not decay. Thus the total amount of waves pertaining to linear degenerate fields is $O(1)TV$. Therefore we differentiate the strength of these two type of waves and set

$$\begin{aligned}
&X_i(t) : \text{amount of } i\text{-waves at time } t,\ i = 1,2,\ldots,n,\\
&X(t) \equiv \sum_{i\in I} X_i(t) \quad \text{amount of waves pertaining to genuinely nonlinear fields at time } t,\\
&\sum_{i=1}^{n} X_i(t) = O(1)TV : \ \text{amount of waves at time } t.
\end{aligned} \tag{5.1}$$

Waves are altered by interactions. There are two types of interactions, interaction among i-waves has third order effects, and interaction between waves of distinct characteristic fields has the second order effects. We monitor the amount of interactions for different regions in the (x,t) space. There is the notion of i-th generalized characteristic curve, which propagates with either shock or characteristic speed. For scalar laws, this is defined first for piecewise continuous solutions and then approximate the general solutions by piecewise continuous solutions. For systems, it is defined through the wave tracing technique of [8]. i-waves do not cross an i-th generalized characteristic curve. For compactly supported initial data, (1.5), the solution at later time is also compactly supported,

$$\begin{aligned} \boldsymbol{u}(x,t) \ &= \boldsymbol{u}_0, \text{ for } |x| > M + C_1 t, \ C_1 \equiv \sup\{\lambda_i(\boldsymbol{u}), \ i = 1, 2, \ldots, n, \} \\ &\quad \text{for all } \boldsymbol{u} \text{ under consideration.} \end{aligned} \tag{5.2}$$

Choose the fixed time $t_0 \geq M$. Through $(\pm(C_1+1)M, t_0)$ draw generalized characteristics $\Gamma_i^{\pm}$. These curves meet before time t_1, Figure 4. The region after time t_1 and between $\Gamma_i^-(t_0)$ and $\Gamma_i^+(t_0)$ is denoted by Ω_i; and the region between Γ_i^+ and Γ_{i+1}^- is denoted by $\bar{\Omega}_i(t_0)$. By strict hyperbolicity,

$$[\lambda] \equiv \min\{|\lambda_j(\boldsymbol{u}_1) - \lambda_k(\boldsymbol{u}_2)|, \ j \neq k, \text{for all } \boldsymbol{u}_1 \text{ and } \boldsymbol{u}_2 \text{ under consideration}\}$$

is positive. Thus these generalized characteristic curves of distinct families intersect before time t_1, Figure 4, and

$$t_1 - t_0 \leq \frac{M + C_1 t_0}{[\lambda]}. \tag{5.3}$$

From the choice of $t_0 \geq M$ and (5.3), we may set

$$t_1 \equiv C_2 t_0, \ C_2 \equiv 1 + \frac{1 + C_1}{[\lambda]} \tag{5.4}$$

By the Glimm estimate, the amount of waves at any time t is $O(1)TV$. Waves pertaining to the linear degenerate fields behave essentially as linear waves and do not decay in time. Waves pertaining to genuinely nonlinear fields are expected to decay in total variation and tends to N-waves in the

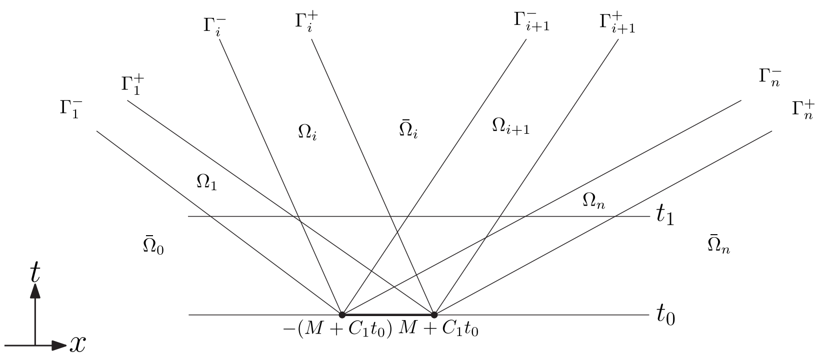

Figure 4: Regions for wave coupling, first step.

$L_1(x)$ norm. Thus we distinguished these nonlinear waves and will monitor their total strength $X(t)$ at time t. Although there are complex wave interactions, it is possible to quantify the concentration of i-waves in primary region Ω_i, and the degree of lacuna of waves in the wake region $\bar{\Omega}_j$. Thus we set

$$\begin{aligned} &X_i(t): \text{ amount of } i\text{-waves at time } t,\ i=1,2,\dots,n;\\ &\bar{X}_i(t_1): \text{ amount of } i\text{-waves at time } t_1 \text{ outside of } \Omega_i,\ \bar{X}(t_1)\equiv\sum_{i=1}^{n}\bar{X}_i(t_1);\\ &X(t)=\sum_{i\in I}X_i(t): \text{ amount of wave pertaining to genuinely nonlinear fields at time } t. \end{aligned} \tag{5.5}$$

Lemma 5.1.

$$\bar{X}(t_1)=O(1)\big((TV)^2+(X(t_0))^3\big); \tag{5.6}$$
$$Q_d(t_1)=O(1)(TV)^3; \tag{5.7}$$
$$Q_s(t_1)=O(1)\big((X(t_0))^3+(TV)^6\big). \tag{5.8}$$

Proof. Note that i-waves, $i\in II$, do not interact among themselves, and the interaction by wave of the same characteristic families are concentrated on i-waves for $i\in I$. Therefore $Q_s(t_0)=O(1)(X(t_0))^3$. Clearly, $Q_d(t_0)=O(1)(TV)^2$. Since points in the region $\bar{\Omega}_i$ are not related by characteristics directly to the support at time t_0, those waves in $\bar{\Omega}_i$ are produced by interaction, and so

$$\bar{X}_i(t_1)=O(1)\big(Q_d(t_0)+Q_s(t_0)\big)=O(1)\big((TV)^2+(X(t_0))^3\big). \tag{5.9}$$

This proves the estimate (5.6).

At time t_1, i-waves in Ω_i do not interact with j-waves in Ω_j for $i\neq j,\ i,j=1,\dots,n$, because they scatter away from each other. Thus there is no contribution to $Q_d(t_0)$ this way, see the definition of $Q_d(J)$ in (4.1). The contribution to $Q_d(t_1)$ therefore comes from waves counted in $\bar{X}_i(t_1)$ with other waves and so from (5.6)

$$Q_d(t_1)=O(1)\sum_{i=1}^{n}\bar{X}_i(t_1)TV=O(1)\big((TV)^2+(X(t_0))^3\big)TV.$$

Note that $X(t_0) = O(1)TV$ and so the above yields the estimate (5.7). Total amount of i-waves at time t_1 is less that at time t_0 plus the interaction and is of the amount of $X(t_0) + O(1)(TV)^2$. The potential interaction of waves of the same genuinely nonlinear characteristic family at time t_1 is therefore of the amount of

$$Q_s(t_1) = \big(X(t_0) + O(1)(TV)^2\big)^3,$$

which yields the estimate (5.8). This completes the proof of the lemma. □

Repeat the above process and draw generalized characteristics from $x = \pm(M + C_1 t_1)$ at time t_1 which intersect before time t_2 and form regions $\Omega_i(t_1)$, $\bar{\Omega}_i(t_1)$, etc, Figure 5. Denote by $\bar{X}_i(t_1)$ the amount of i-waves outside of $\Omega(t_1)$, etc. Inductively, we then obtain a sequence of increasing times $t_m \equiv (C_2)^m t_0,\ m = 1, 2, \ldots$.

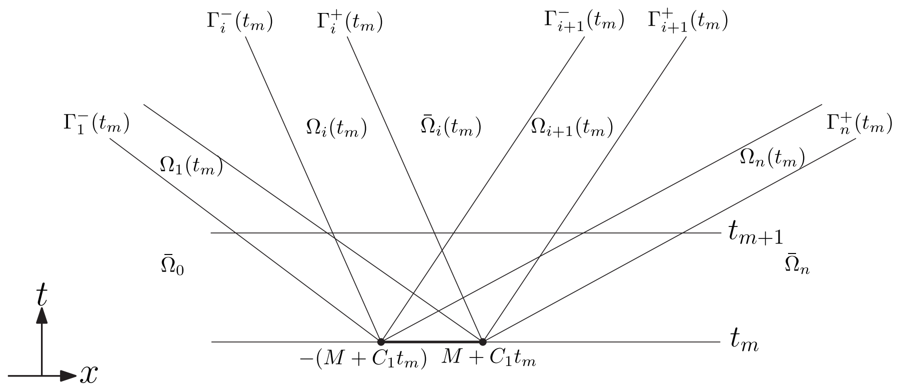

Figure 5: Regions for wave coupling, m-th step.

Proposition 5.2. *For sufficiently small* TV*,*

$$\bar{X}(t_m)=O(1)\Big(\sum_{i=0}^{m-1}(TV)^{m-i-1}(X(t_i))^3+(TV)^{m+1}\Big), m=1,2,\ldots; \tag{5.10}$$

$$Q_d(t_m) + Q_s(t_m)=O(1)\Big(\sum_{i=0}^{m}(TV)^{m-i}(X(t_i))^3+(TV)^{m+2}\Big), m=0,1,2,\ldots. \tag{5.11}$$

Moreover,

$$\boldsymbol{u}(x,t) = \boldsymbol{u}_0 + O(1)\big(Q_d(t_m) + Q_s(t_m)\big) + O(1)(X(t_m))^3, \quad \textit{for } (x,t) \in \bar{\Omega}_i(t_m),\ i = 1, 2, \ldots, n-1. \tag{5.12}$$

Proof. By the same reasoning as in Lemma 5.1,

$$Q_d(t_m) = O(1)TV \cdot \bar{X}(t_m),\ Q_s(t_m) = O(1)(X(t_m))^3, \tag{5.13}$$

and

$$\bar{X}(t_m) = O(1)\big(Q_d(t_{m-1}) + Q_s(t_{m-1})\big). \tag{5.14}$$

With (5.13) and (5.14), the estimates (5.11) and (5.11) are easily proved by induction in m, with the initial case of $m = 1$ done in Lemma 5.1.

The solution variation in $\bar{\Omega}_i(t_m)$ is of the order of $\bar{X}_i(t_m) = O(1)\big(Q_d(t_{m-1}) + Q_s(t_{m-1})\big)$ and so

$$\boldsymbol{u}(x_1, t_1) - \boldsymbol{u}(x_2, t_2) = O(1)\big(Q_d(t_{m-1}) + Q_s(t_{m-1})\big),$$
$$\text{for any } (x_1, t_1),\ (x_2, t_2) \in \bar{\Omega}_i(t_m).$$

For $(x, t) \in \Omega_i(t_m),\ i \in I$, besides the amount $X(t_m)$ of i-waves, there are other waves of the amount of $\bar{X}(t_m)$. By Theorem 3.2, the i-waves lie on the i-characteristic curve $\boldsymbol{R}_i$ except for a third order error. Thus, for any fixed $(x, t) \in \Omega_i(t_m)$,

$$\boldsymbol{u}(x_1, t_1) \in \boldsymbol{R}_i(\boldsymbol{u}(x, t)) + O(1)\big(((X(t_m))^3 + Q_d(t_{m-1}) + Q_s(t_{m-1})\big),$$
$$\text{for any } (x_1, t_1) \in \Omega_i(t_m),\ i \in I.$$

For $i \in II$, the wave curve $\boldsymbol{W}_i(\boldsymbol{u}_0) = \boldsymbol{R}_i(\boldsymbol{u}_0)$ and their is no third order error as for the genuinely nonlinear case above:

$$\boldsymbol{u}(x_1, t_1) \in \boldsymbol{R}_i(\boldsymbol{u}(x, t)) + O(1)\big(Q_d(t_{m-1}) + Q_s(t_{m-1})\big),$$
$$\text{for any } (x_1, t_1) \in \Omega_i(t_m),\ i \in II.$$

These two estimates and that $\boldsymbol{u}(x, t) = \boldsymbol{u}_0$ for (x, t) in $\bar{\Omega}_0$ and in $\bar{\Omega}_n$ imply the estimate (5.12). This completes the proof of the proposition. □

Remark 5.3. For 2×2 conservation laws, there exist the Riemann invariant coordinates and when the strength of waves is measured in the Riemann invariant coordinates, the wave interaction measure Q_d is also third order, same order as for Q_s. This is sufficient for the analysis of decay and convergence to N-waves. The decay of solutions were done in an unpublished note related to Glimm-Lax [5], and convergence to N-waves done in DiPerna [1]. The analysis of N-waves using the Riemann invariant coordinates is replaced by the derivation of the inviscid Burgers equation for the characteristic speed in [9], (2.5), which is the natural setting for general systems. For systems with more than two equations, Q_d is second order in general. Neverthelss, if the system is genuinely nonlinear, the estimates in Lemma 5.1, when repeated to time t_2, are simplified to

$$\bar{X}(t_2) + Q_d(t_2) + Q_s(t_2) = O(1)(X(t_0))^3. \tag{5.15}$$

For any given t_0, we have $t_2 = (C_2)^2 t_0$, and so t_2 and t_0 are of the same order. This is sufficient for the decay and convergence to N-wave analysis in [9]. The analysis in [12] is to obtain pointwise estimate and to improve the convergence rate, under the same setting as [9].

The above analysis do not apply to systems with linearly degenerate modes. The Euler equations in gas dynamics consist of two genuinely nonlinear acoustic modes and one linearly degenerate thermal mode. For magnetohydrodynamics equations, there is an additional linearly degenerate Alfv́en mode. Linear degenerate modes also occur in elastic models. Our present aim is to study the N-waves for the genuinely nonlinear modes within the system containing also linearly degenerate modes. For this, we carry out the repeated decoupling analysis in Proposition 5.2 to gain decay for the wave interaction potential, see also Proposition 5.4 below.

Proposition 5.4. *Suppose the total strength of waves pertaining to genuinely nonlinear fields decays at the same rate as for the N-waves:*

$$X(t) = O(1)TV \cdot t^{-1/2},\ t \geq 1. \tag{5.16}$$

Then the wave interaction potentials decay at the same rate as $(X(t))^3$:

$$Q_d(t) + Q_s(t) = O(1)(TV)^3 t^{-\frac{3}{2}},\ t \geq (C_2)^2 M. \tag{5.17}$$

Proof. From (5.11),

$$Q_d((C_2)^m t_0)+Q_s((C_2)^m t_0) = O(1)\Big(\sum_{i=0}^{m}(TV)^{m-i+3}\big((C_2)^i t_0\big)^{-\frac{3}{2}}+(TV)^{m+2}\Big). \tag{5.18}$$

For any given $t \geq (C_2)^2 M$, there exists m such that

$$(C_2)^m \leq \frac{t}{M} \leq (C_2)^{m+1}, \text{ for some integer } m \geq 2,$$

and set

$$t_0 \equiv \frac{t}{(C_2)^m}, \text{ so that } t = (C_2)^m t_0, \text{ and } M \leq t_0 \leq C_2 M.$$

Then (5.18) becomes

$$\begin{aligned} Q_d(t) + Q_s(t) &= O(1)(TV)^3 t^{-\frac{3}{2}} \Big(\sum_{i=0}^{m} \big(TV \cdot (C_2)^{\frac{3}{2}}\big)^{m-i} + (TV)^{m-1} (C_2)^{\frac{3m}{2}} t_0^{\frac{3}{2}} \Big) \\ &= O(1)(TV)^3 t^{-\frac{3}{2}}. \end{aligned}$$

This proves (5.17). □

6. Expansion of Rarefaction Waves

Waves pertaining to a genuinely nonlinear i-characteristic field, $i \in I$, decay because of cancellation of shock and rarefaction waves. This is due to the expansion of rarefaction waves and the compression of shock waves. This basic mechanism is quantitatively expressed in the following proposition on the expansion rate of the rarefaction waves, [5], [11].

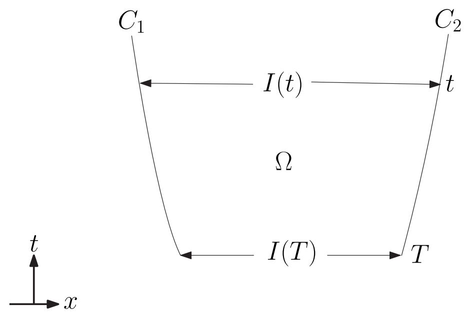

Figure 6: Expansion of rarefaction waves.

Consider a genuinely nonlinear i-characteristic field, $i \in I$. Draw two generalized i-th characteristics C_- to the left and C_+ to the right from the initial time T. Let $I(t)$ be the interval between them at time t, and Ω the region between C_1, C_2, time T, and time t. Denote by $X_+(t)$ the total amount of i-rarefaction waves on the interval $I(t)$ at time t between C_- and C_+, and $\tilde{X}(T,t)$ the total amount of j-waves, $j \neq i$ crossing $I(T)$ or C_-, C_+ between time T and time t. Denote by Ω the region between C_1, C_2, time t_0 and time t, Figure 6.

Proposition 6.1.

$$X_+(t) \leq \frac{I(t)}{t-T}\big(1 + O(1)\tilde{X}(T,t) + O(1)D(\Omega)\big) + O(1)D(\Omega). \tag{6.1}$$

The estimate (6.1) registers the linear expansion rate of the rarefaction waves, with the coupling effects of $D(\Omega)$ and $\tilde{X}(T,t)$.

7. Decay of Solution

Before studying the time-asymptotic behavior of solutions in the next two sections, we first study the decay of total strength $X(t)$ of waves for genuinely nonlinear fields and the wave interaction potential $Q_d(t) + Q_s(t)$.

Theorem 7.1. *Consider the solution of system of conservation laws with small initial total variation TV constructed by Glimm scheme. Then, as $t \to \infty$, the total strength $X(t)$ of waves pertaining to genuinely nonlinear fields decays at the rate of $t^{-1/2}$:*

$$X(t) = O(1)TV(t+1)^{-\frac{1}{2}} \tag{7.1}$$

and the amount of potential wave interactions decays at the rate of $t^{-3/2}$:

$$Q_d(t) + Q_s(t) = O(1)(TV)^3(t+1)^{-\frac{3}{2}}. \tag{7.2}$$

Morevoer,

$$\boldsymbol{u}(x,t) = \boldsymbol{u}_0 + O(1)(TV)^3(t+1)^{-\frac{3}{2}} \text{ for } (x,t) \in \tilde{\Omega}_i,\ i = 1, 2, \dots. \tag{7.3}$$

Proof. It follows from Proposition 5.4 that estimate (7.1) implies estimate (7.2). Thus we may set up the induction process for verifying (7.1). The main step in the induction process is using the estimate (6.1) on the expansion waves to establish estimate (7.1) from estimate (7.2). This general approach is carried out as follows:

Consider the process (5.2)-(5.4), Figure 4, and let t_0 be any given time and set $t_1 = T$. Let $i \in I$ be a genuinely nonlinear field. Through the edge of support at time t_0 draw i-characteristics $C_\pm = \Gamma_i^\pm$ and denote by $\Omega = \Omega_i$ the region between time $t = T$ and $C_\pm$. We have from (6.1)

$$X_+(t) \leq \frac{I(t)}{t-T}\big(1 + O(1)\tilde{X}(T,t) + O(1)D(\Omega)\big) + O(1)D(\Omega). \tag{7.4}$$

Here $I(t)$ is the distance between C_- and C_+ at time t, Figure 7, $X_+(t)$ is the amount of i-th rarefaction waves in Ω at time t, and $\tilde{X}(T,t)$ the amount of j-waves, $j \neq i$, crossing $I(T)$ and $C_\pm$ between times T and t.

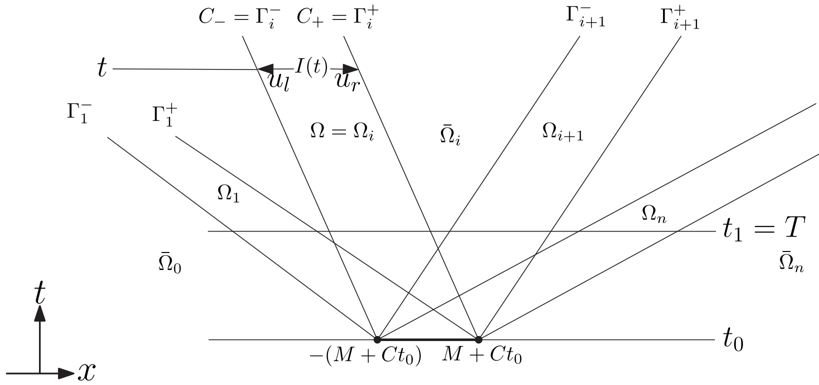

Figure 7: Wave expansion and decay.

By (4.3), the amount of wave interactions $D(\Omega)$ in Ω is bounded by $Q_d(T) + Q_s(T)$:

$$D(\Omega) = O(1)\big(Q_d(T) + Q_s(T)\big) = O(1)\big(Q_d(t_0) + Q_s(t_0)\big). \tag{7.5}$$

The amount $\tilde{X}(T,t)$ of j-waves, $j \neq i$, crossing the boundary of Ω belong to those produced by interaction after time t_0:

$$\tilde{X}(T,t) = O(1)D(t_0) = O(1)\big(Q_d(t_0) + Q_s(t_0)\big). \tag{7.6}$$

By (7.5) and (7.6), (7.4) becomes

$$X_+(t) \leq \frac{I(t)}{t-T}\big(1 + O(1)\big(Q_d(t_0) + Q_s(t_0)\big)\big) + O(1)\big(Q_d(t_0) + Q_s(t_0)\big). \tag{7.7}$$

Following the proof of (5.12) in Proposition 5.2, we have

$$\boldsymbol{u}(x,t) = \boldsymbol{u}_0 + O(1)\big(Q_d(t_0) + Q_s(t_0) + (X(T))^3\big),$$
$$\text{for } (x,t) \in \bar{\Omega}_j,\ j = 1, 2, \ldots, n-1. \tag{7.8}$$

Denote by $\boldsymbol{u}_l$ (or $\boldsymbol{u}_r$) the solution evaluated at the right side of C_- (or left side of C_+) at time t and write

$$\lambda_0 \equiv \lambda_i(\boldsymbol{u}_0),\ \lambda_l \equiv \lambda_i(\boldsymbol{u}_l),\ \lambda_r \equiv \lambda_i(\boldsymbol{u}_r).$$

The distance $I(t)$ is governed by the Rankine-Hugoniot condition. From Theorem 3.2, the speed of C_- (or C_+) is approximated by the arithmetic mean of the characteristic speeds $\lambda_l,\ (or \lambda_r)$ and λ_0 with perturbation of the order of $O(1)(Q_d(t_0) + Q_s(t_0) + (X(T))^3)$. Thus we have from the estimate (7.8),

$$\begin{aligned}&\frac{d}{dt}I(t)\\ &= O(1)\big(Q_d(t_0)+Q_s(t_0)+(X(T))^3\big)+\frac{\lambda_r-\lambda_l}{2}+O(1)\big((\lambda_r-\lambda_0)^2-(\lambda_l-\lambda_0)^2\big)\\ &= \big(\frac{1}{2}+O(1)X_i(T)\big)(\lambda_r-\lambda_l)+O(1)\big(Q_d(t_0)+Q_s(t_0)+(X(T))^3\big).\end{aligned} \tag{7.9}$$

The difference $\lambda_r - \lambda_l$ is $X_+(t)$ minus the amount of i-th shock waves between C_- and C_+, with the perturbation of waves of other families. The latter is of the amount of $O(1)(Q_d(t_0) + Q_s(t_0))$. Moreover, from (7.8), $X_+(t) = X_i(t)/2 + O(1)(Q_d(t_0) + Q_s(t_0))$. Thus we have

$$\lambda_r - \lambda_l \le X_+(t) + O(1)(Q_d(t_0) + Q_s(t_0)) = \frac{X_i(t)}{2} + O(1)(Q_d(t_0) + Q_s(t_0)).$$

These, (7.7) and (7.9) yield:

$$\frac{d}{dt}I(t) \le \big(\frac{1}{2}+O(1)X(T)\big)\frac{I(t)}{t-T}+O(1)(Q_d(t_0)+Q_s(t_0)+(X(T))^3\big); \tag{7.10}$$
$$\frac{d}{dt}I(t) \le \big(\frac{1}{4}+O(1)X(T)\big)X_i(t)+O(1)(Q_d(t_0)+Q_s(t_0)+(X(T))^3\big). \tag{7.11}$$

We now start the induction process. To goal is to show

$$X_i(t) \le H_n t^{-\frac{1}{2}},\ \text{for } t < T_m \equiv 2^m T_0,\ m = 0, 1, 2, \ldots, \tag{7.12}$$

where

$$T_0 = \varepsilon^{-\frac{11}{5}} M, \ H_0 \equiv \varepsilon^{-\frac{1}{10}} M^{\frac{1}{2}}, \ \varepsilon \equiv 2TV. \tag{7.13}$$

Since $\gamma_0 \equiv H_0(T_0)^{-\frac{1}{2}} = \varepsilon$, we see that (7.12) holds for $m = 0$. Assume that (7.12) holds for $m \leq p$ with the coefficients $H_m, \ m = 0, 1 \cdots, p$, satisfying

$$H_0 \leq H_1 \leq \cdots \leq H_p \leq 2H_0.$$

As mentioned at the beginning of this proof, it follows from Proposition 5.4 that estimate (7.1) implies estimate (7.2). Thus the induction hypothesis implies

$$X_i(t) \leq H_p t^{-\frac{1}{2}}, \ Q_d(t) + Q_s(t) + (X(t))^3 = O(1)(H_p)^3 t^{-\frac{3}{2}}, \text{ for } t < T_p. \tag{7.14}$$

We now apply the set up above with

$$t_0 = (H_p T_p)^{\frac{2}{5}}, \ \gamma_p \equiv H_p (t_0)^{-\frac{1}{2}}.$$

From the induction hypothesis,

$$X(t_0) \leq \gamma_p.$$

Integrate (7.10) from $t = T$ to $t = T_p$, making use of (7.14),

$$I(T_p) \leq \frac{1}{2}(1 + O(1)\gamma_p) H_p((T_p)^{\frac{1}{2}} - T^{\frac{1}{2}}) + O(1)(\gamma_p)^3 (T_p - T) + I(T).$$

Next integrate (7.11) for $t \in (T_p, T_{p+1})$:

$$I(t) \leq (\frac{t - T}{T_p - T})^{\frac{1}{2} + O(1)\gamma_p} I(T_p) + O(1)(\gamma_p)^3 (t - T).$$

Noting that $I(T) = O(1)T = O(1)t_0$, we have from the above two estimates

$$I(t) \leq (\frac{t - T}{T_p - T})^{\frac{1}{2} + O(1)\gamma_p} \Big(\frac{1}{2}(1 + O(1)\gamma_p) H_p ((T_p)^{\frac{1}{2}} - T^{\frac{1}{2}}) + O(1)(\gamma_p)^3 (T_p - T) + O(1) t_0 \Big) + O(1)(\gamma_p)^3 (t - T). \tag{7.15}$$

We conclude from (7.7), (7.8), and (7.15) that

$$X_i(t) \le (\frac{t-Ct_0}{T_p-T})^{O(1)\gamma_p}(t-Ct_0)^{-\frac{1}{2}}$$
$$\cdot\Big((1+O(1)\gamma_p)H_p\frac{(T_p)^{\frac{1}{2}}T^{\frac{1}{2}}}{(T_p-T)^{\frac{1}{2}}}+O(1)\frac{T}{(T_p-T)^{\frac{1}{2}}}\Big)+O(1)(\gamma_p)^3. \quad (7.16)$$

The induction is complete if H_{p+1} is found to satisfy

$$(\frac{t-T}{T_p-T})^{O(1)\gamma_p}(t-T)^{-\frac{1}{2}}[(1+O(1)\gamma_p)H_p\frac{(T_p)^{\frac{1}{2}}(Ct_0)^{\frac{1}{2}}}{(T_p-T)^{\frac{1}{2}}}$$
$$+O(1)\frac{T}{(T_p-T)^{\frac{1}{2}}}]+O(1)(\gamma_p)^3 \le H_{p+1}t^{-\frac{1}{2}},\ \text{for } t\in(T_p,T_{p+1}).$$

This is so if

$$H_{p+1} \ge (\frac{2T_p-T}{T_p-T})^{O(1)\gamma_p}(\frac{T_p}{T_p-T})^{\frac{1}{2}}[(1+O(1)\gamma_p)H_p\frac{(T_p)^{\frac{1}{2}}T^{\frac{1}{2}}}{(T_p-T)^{\frac{1}{2}}}$$
$$+O(1)\frac{T}{(T_p-T)^{\frac{1}{2}}}]+O(1)(\gamma_p)^3. \quad (7.17)$$

We assert that this can be satisfied with a choice of H_{p+1} having the property

$$H_0=\varepsilon^{-\frac{1}{10}}M \le H_p \le H_{p+1} \le H_p 3^{O(1)\gamma_p}(1+O(1)\gamma_p)+O(1)2^{-\frac{p}{10}}\varepsilon^{\frac{1}{5}} \le 2H_0. \quad (7.18)$$

This is the consequence of the following simple estimates. From the definition

$$T_0 \equiv \varepsilon^{-\frac{11}{5}}M,\ H_0=\varepsilon^{-\frac{1}{10}}M^{\frac{1}{2}},\ T_p\equiv 2^pT_0,\ t_0\equiv(H_pT_p)^{\frac{2}{5}},\ \gamma_p=H_p(t_0)^{-\frac{1}{2}}$$

we deduce that

$$\frac{\gamma_p}{\gamma_{p-1}}=2^{-\frac{1}{5}}(\frac{H_p}{H_{p-1}})^{\frac{4}{5}} \le 2^{-\frac{1}{10}}$$

where the last inequality comes from the estimate in (7.18) that we have assumed. Thus

$$\gamma_p \le 2^{-\frac{p}{10}}\gamma_0=\varepsilon 2^{-\frac{p}{10}},$$

which is small and decaying exponentially in p. With this it is easy to see that (7.18) should hold if the terms not related to γ_p on the right hand side of (7.17) can be satisfied for the small ε. The basic estimate for this is the ratio

$$\frac{t_0}{T_p} = (T_p)^{-\frac{3}{5}}(H_p)^{\frac{2}{5}} \leq 22^{-\frac{3p}{5}}T_0H_0 = 2^{\frac{3p}{5}}(\varepsilon^{\frac{11}{5}}M)^{-\frac{3}{5}}(\varepsilon^{-\frac{1}{10}}M^{\frac{1}{2}})^{\frac{2}{5}}$$
$$= M^{-\frac{2}{5}}2^{-\frac{3p}{5}}\varepsilon^{\frac{31}{25}},$$

which is small and tends to zero exponentially in p. For instance, it implies the first ratio on the right hand side of (7.18)

$$\frac{2T_p - T}{T_p - T} \leq 3.$$

The other terms on the right hand side of (7.18) are estimated similarly. This completes the proof of the theorem. □

8. N-waves

With the decay of the total variation of the solution, one can study in more detail the wave distribution and in particular the convergence to N-waves and linear waves. This section studies the convergence to N-waves. Recall from (1.9) that the (x, t) space is divided into regions

$$\tilde{\Omega}_1 \equiv \{(x,t):\ x < \tilde{\lambda}_1 t\},\ \tilde{\Omega}_n \equiv \{(x,t):\ x > \tilde{\lambda}_{n-1}t\},$$
$$\tilde{\Omega}_i \equiv \{(x,t):\ \tilde{\lambda}_{i-1}t < x < \tilde{\lambda}_i t\},\ i = 2, \dots, n-1,$$

with the constants $\tilde{\lambda}_i,\ i = 1, \dots, n-1$ chosen such that

$$\lambda_i(\boldsymbol{u}) < \tilde{\lambda}_i < \lambda_{i+1}(\boldsymbol{u}) \text{ for all states } \boldsymbol{u} \text{ under consideration.}$$

Theorem 8.1. *For each i-th genuinely nonlinear characteristic field, $i \in I$, there exist two time invariants p_i, q_i so that the solution of* (1.5) *converges to the N-wave $\boldsymbol{N}_i(x,t) = N_{p_i,q_i}(x - \lambda_i(\boldsymbol{u}_0)t, t)\boldsymbol{r}_i(\boldsymbol{u}_0)$ in $\tilde{\Omega}_i$. There is an explicit description of the solution,* (8.9)*, which yields that the convergence rate of the solution in $\tilde{\Omega}_i$ to the $\boldsymbol{N}_i(x,t)$ is of the rate of $t^{-1/4}$ in $L_1(x)$.*

Proof. For a given time t, set $t_0 = t^{\frac{2}{5}},\ t_2 = (C_2)^2 t_0 < t$ and follow the set-up of Proposition 5.2. Consider generalized characteristics $\bar{\Gamma}_i^- :\ x = x_l(t)$, and $\bar{\Gamma}_i^+ :\ x = x_r(t)$, Figure 7. Consider the lines separating the characteristics:

$$\Gamma_j \equiv \{(x,t):\ x=\mu_j t,\ \mu_j \equiv \frac{\lambda_j(\boldsymbol{u}_0)+\lambda_{j+1}(\boldsymbol{u}_0)}{2}\},\ j=1,\dots,n-1;$$
$$\Gamma_0 \equiv \{(x,t):\ x=(\lambda_1(\boldsymbol{u}_0)-1)t\},\ \Gamma_n \equiv \{(x,t):\ x=(\lambda_n(\boldsymbol{u}_0)+1)t\}.$$

After finite time $O(1)M$, the support of the solution is contained in the region between Γ_0 and Γ_n.

In the region between Γ_{i-1} and Γ_i, $\mu_{i-1}t < x < \mu_i t$, we have from Theorem 7.1 that the amount of i-waves decays at the rate of $t^{-1/2}$, and the amount of j-waves, $j \neq i$, decays at the rate of $t^{-3/2}$. Moreover, by Theorem 7.1 and (7.8), along Γ_{i-1} and Γ_i, $\boldsymbol{u}=\boldsymbol{u}_0+O(1)t^{-3/2}$. This implies that, in the weak sense, the solution is governed accurately by the Hopf equation:

$$\lambda_t + (\frac{\lambda^2}{2})_x = \nu^i(x,t),\ \lambda \equiv \lambda_i(\boldsymbol{u}) - \lambda_0 t,\ \lambda_0 \equiv \lambda_i(\boldsymbol{u}_0).$$

The measure $\int \nu^i(x,t)dx$ comes from two sources, the first is the amount of j-waves, $j \neq i$, which is of the order $t^{-3/2}$ as just noted, and the second is due to the fact that i-shock waves do not exactly satisfy the inviscid Burgers equation, there is a third order error $(t^{-1/2})^3 = t^{-3/2}$, Section 3. Thus we have

$$\int_t^\infty \int_{\mu_{i-1}t}^{\mu_i t} \nu^i(x,s)dxds = O(1)(TV)^2 t^{-\frac{1}{2}}.$$

The inviscid Burgers equation has two time invariants, [6], so the above approximate inviscid Burgers equation yields two time invariants time-asymptotically, e.g. (1.7):

$$\begin{aligned} p_i &= \inf_x \int_{\mu_{i-1}t}^{x} [\lambda(x,t)-\lambda_0]dx + O(1)(TV)^2 t^{-\frac{1}{2}}, \\ q_i &= \max_x \int_x^{\mu_i t} [\lambda(x,t)-\lambda_0]dx + O(1)(TV)^2 t^{-\frac{1}{2}},\ \lambda_0 \equiv \lambda_i(\boldsymbol{u}_0). \end{aligned} \tag{8.1}$$

Draw generalized i-characteristics $x=x_l(t)$ and $x=x_r(t)$ starting at time $t^{2/5}$, Figure 8. Draw a backward characteristic through a location (x,t), $x_l(t) < x < x_r(t)$, to reach the time $t^{2/5}$ at x_0. The change of speed of the backward characteristic after time s due to waves crossing it is of the

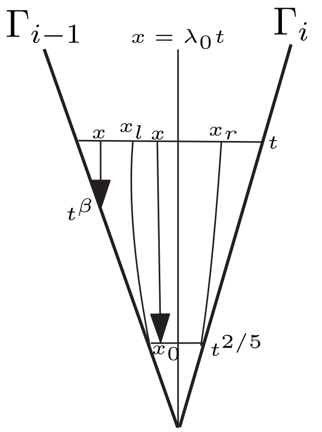

Figure 8: Wave distribution for a genuinely nonlinear field.

order of $O(1)(TV)^2(s+1)^{-3/2}$, and so its location at time t is

$$\begin{aligned} x &= x_0 + \int_{t^{\frac{2}{5}}}^{t} \big(\lambda_i(x,t) + O(1)(TV)^2(s+1)^{-\frac{3}{2}}\big)ds \\ &= \lambda_i(x,t)(t - t^{\frac{2}{5}}) + O(1)(TV)^2(t+1)^{-\frac{1}{5}} = x_0 + \lambda_i(x,t)t + O(1)t^{\frac{2}{5}}. \end{aligned}$$

Since $x_0 = \lambda_0 t + O(1)t^{\frac{2}{5}}$, this implies that the solution is close to the centered i-rarefaction wave for $x_l(t) < x < x_r(t)$, see (7.5),

$$\lambda_i(x,t) = \frac{x - \lambda_0 t}{t} + O(1)t^{-\frac{3}{5}}, \ \boldsymbol{u}(x,t) = \boldsymbol{u}_0 + O(1)t^{-\frac{3}{2}}. \tag{8.2}$$

Next consider the region left of the generalized characteristic, $\mu_{i-1}t < x < x_l(t)$, and draw a backward i-characteristic to meet the boundary at time t^β for some β, $2/5 < \beta < 1$, Figure 8. The speed of the backward characteristic changes due to waves crossing it, which is of the order of $(TV)^3(t^\beta)^{-3/2} = t^{-3\beta/2}$. The end speed $\lambda_i(x,t) = \lambda_0 + O(1)(TV)^3 t^{-3\beta/2}$, by (7.8). Thus

$$\begin{aligned} x &= \mu_{i-1}t^\beta + (t - t^\beta)\big(\lambda_0 + O(1)(TV)^3 t^{-\frac{3\beta}{2}}\big); \text{ or} \\ \lambda_0 t - x &= (\lambda_0 - \mu_{i-1})t^\beta + O(1)(TV)^3 t^{1-\frac{3\beta}{2}}. \end{aligned}$$

Since $\lambda_0 - \mu_{i-1}$ is positive and of order one and since $\beta \geq 2/5$ and TV is small, we have $\beta > 1 - 3\beta/2$. Thus the above shows that

$$C_1 t^{\beta} \leq \lambda_0 t - x \leq C_2 t^{\beta},$$

for some positive constant $C_1 < C_2$. In particular, there exist $5/2 \leq \beta_l,\ \beta_r \leq 1$,

$$C_1 t^{\beta_l} \leq \lambda_0 t - x_l(t) \leq C_2 t^{\beta_l},\ C_1 t^{\beta_r} \leq x_r(t) - \lambda_0 t \leq C_2 t^{\beta_r}. \tag{8.3}$$

The waves for the interval $(\mu_{i-1}t, x)$ are those produced after time t^{β} and so have total strength $O(1)(TV)^3 t^{-3\beta/2}$, which is of the order of $O(1)(TV)^3(\lambda_0 t - x)^{-3/2}$. Similar estimate holds for the region $x_r(t) < x < \mu_i t$ and we have thus shown that

$$\begin{aligned} \boldsymbol{u}(x,t) = \boldsymbol{u}_0 + O(1)(TV)^3 |x - \lambda_0 t|^{-\frac{3}{2}}, \\ \text{for } \mu_{i-1}t < x < x_l(t),\ x_r(t) < x < \mu_i t. \end{aligned} \tag{8.4}$$

From (8.2) and (8.4),

$$\lambda_i(x,t) = \lambda_0 + \begin{cases} O(1)(TV)^3 |x - \lambda_0 t|^{-\frac{3}{2}}, \text{ for } \mu_{i-1}t < x < x_l(t), \\ \frac{x - \lambda_0 t}{t} + O(1)(TV)^3 t^{-\frac{3}{5}},, \text{ for } x_l(t) < x < x_r(t), \\ O(1)(TV)^3 |x - \lambda_0 t|^{-\frac{3}{2}}, \text{ for } x_r(t) < x < \mu_i t. \end{cases} \tag{8.5}$$

We use this and (8.3) to relate the location of the two generalized characteristics $x = x_l(t)$ and $x = x_r(t)$ to the time invariants p_i, q_i given in (8.1). In view of the decay property $\boldsymbol{u}(x,t) - \boldsymbol{u}_0 = O(1)TV(1+t)^{-1/2}$ in Theorem 7.1, the second equation in (8.5) implies that

$$|x_l(t) - \lambda_0 t| + |x_r(t) - \lambda_0 t| = O(1)TV(t+1)^{\frac{1}{2}}. \tag{8.6}$$

The integrations outside the generalized characteristics are time-decaying and do not contribute to time invariants p_i, q_i:

$$\int_{\mu_{i-1}t}^{x_l(t)} (\lambda_i(x,t) - \lambda_0)dx = O(1)(TV)^3 |x_l(t) - \lambda_0 t|^{-\frac{1}{2}} = O(1)(TV)^3 t^{-\beta_l/2},$$
$$\int_{x_r(t)}^{\mu_i t} (\lambda_i(x,t) - \lambda_0)dx = O(1)(TV)^3 |x_r(t) - \lambda_0 t|^{-\frac{1}{2}} = O(1)(TV)^3 t^{-\beta_r/2}.$$

The integrations between the generalized characteristics are:

$$\int_{x_l(t)}^{\lambda_0 t}(\lambda_i(x,t)-\lambda_0)dx = -\frac{1}{2t}\big(\lambda_0 t - x_l(t)\big)^2 + O(1)(TV)^3 t^{-\frac{3}{5}}\big(\lambda_0 t - \mu_{i-1}t\big),$$
$$\int_{x_l(t)}^{\lambda_0 t}(\lambda_i(x,t)-\lambda_0)dx = \frac{1}{2t}\big(\lambda_0 t - x_r(t)t\big)^2 + O(1)(TV)^3 t^{-\frac{3}{5}}\big(\lambda_0 t - \mu_{i-1}t\big).$$

This and (8.6) yields

$$\int_{x_l(t)}^{\lambda_0 t}(\lambda_i(x,t)-\lambda_0)dx = -\frac{1}{2t}\big(\lambda_0 t - x_l(t)\big)^2 + O(1)(TV)^3 t^{-\frac{1}{10}},$$
$$\int_{x_l(t)}^{\lambda_0 t}(\lambda_i(x,t)-\lambda_0)dx = \frac{1}{2t}\big(\lambda_0 t - x_r(t)\big)^2 + O(1)(TV)^3 t^{-\frac{1}{10}}.$$

The above analysis also shows that

$$\inf_x \int_{\mu_{i-1}t}^{x}[\lambda(x,t)-\lambda_0]dx = -\frac{1}{2t}\big(\lambda_0 t - x_l(t)\big)^2 + O(1)(TV)^3 t^{-\frac{1}{10}},$$
$$\max_x \int_{x}^{\mu_i t}[\lambda(x,t)-\lambda_0]dx = \frac{1}{2t}\big(\lambda_0 t - x_r(t)\big)^2 + O(1)(TV)^3 t^{-\frac{1}{10}}.$$

This and (8.1) for the time invariants p_i, q_i gives the estimate of the location of the generalized characteristics:

$$\begin{aligned}\lambda_0 t - x_l(t) &= \sqrt{-2p_i t} + O(1)(TV)^3 t^{-\frac{1}{10}},\\ x_r(t) - \lambda_0 t &= \sqrt{2q_i t} + O(1)(TV)^3 t^{-\frac{1}{10}}.\end{aligned} \tag{8.7}$$

Consider the generic case of $p < 0 < q$. From (8.5) and (8.7), we see that two relatively strong shock waves eventually emerge on the generalized characteristics

$$\begin{aligned}\lambda_i(x_l(t)-0,t) - \lambda_i(x_l(t)+0,t) &= \sqrt{\frac{-2p}{t}} + O(1)(TV)^3 t^{-\frac{3}{5}},\\ \lambda_i(x_r(t)-0,t) - \lambda_i(x_r(t)+0,t) &= \sqrt{\frac{2q}{t}} + O(1)(TV)^3 t^{-\frac{3}{5}}.\end{aligned} \tag{8.8}$$

After the emergence of the two relatively strong shocks, say after time T, we may redo the above analysis as follows: Let C_l and C_r be the generalized characteristics through $(\mu_{i-1}T, T)$ and $(\mu_i T, T)$ which eventually coincide with the two relatively strong shock curves after some finite time $T_1 > T$.

For $(x,t),\ t>T_1$, between C_l and C_r draw backward characteristic to meet time T_1 at (x_0,T_1) between C_l and C_r. The backward characteristic has speed $\lambda_i(x,t)+O(1)(TV)^3(s+1)^{-3/2},\ T_1<s<t$, and so

$$x=x_0+\int_{T_1}^{t}\big(\lambda_i(x,t)+O(1)(TV)^3(s+1)^{-3/2}\big)ds=\lambda_i(x,t)t+O(1).$$

This improves the second estimate of (8.5). For (x,t) between Γ_{i-1} and Γ_i, but outside of C_l and C_r, we also repeat the process before, and we conclude from the above, (8.5) and (8.7) that

$$\begin{aligned}&\lambda_i(x,t)-\lambda_0\\ &=\begin{cases}O(1)(TV)^3|\lambda_0t-x|^{-\frac{3}{2}},\ \text{for}\ \mu_{i-1}t<x-\lambda_0t<-\sqrt{\frac{-2p_i}{t}},\\ \frac{x-\lambda_0t}{t}+O(1)(TV)^3t^{-1},\ \text{for}\ -\sqrt{\frac{-2p_i}{t}}<x-\lambda_0t<\sqrt{\frac{2q_i}{t}},\\ O(1)(TV)^3|x-\lambda_0t|^{-\frac{3}{2}},\ \text{for}\ \sqrt{\frac{2q_i}{t}}<x-\lambda_0t<\mu_it.\end{cases}\end{aligned}\tag{8.9}$$

This completes the description of the solution between Γ_{i-1} and Γ_i. By direct calculations using (8.9),

$$\int_{\mu_{i-1}t}^{\mu_it}|\lambda_i(x,t)-\lambda_0-N(x-\lambda_0t,t;p,q)(x,t)|Dx=O(1)(t+1)^{-\frac{1}{4}}.\tag{8.10}$$

This completes the proof of the theorem. □

9. Linear Waves

For a linearly degenerate i-th field, $i\in II$, the solution $\boldsymbol{u}(x,t),\ (x,t)\in\tilde{\Omega}_i$, tends, time-asymptotically, to a linear i-the simple wave, (2.9). The asymptotic profile depends on the initial data $\boldsymbol{u}(x,0)$. The convergence rate is better than that for the N-waves in Theorem 8.1. To describe the linear wave which dominates the solution in $\tilde{\Omega}_i$, consider a stationary wave $\phi(x)$ and the corresponding i-th simple wave $\boldsymbol{\phi}(x,t)$ is constructed by parametrizing the i-th characteristic curve $\boldsymbol{R}_i(\boldsymbol{u}_0)$ by a non-singular parameter τ with $\tau(\boldsymbol{u}_0)=0$ and set, (2.9),

$$\boldsymbol{\phi}(x,t)\in\boldsymbol{R}_i(\boldsymbol{u}_0),\ \tau(\boldsymbol{\phi}(x,t))=\phi(x-\lambda_i(\boldsymbol{u}_0t).\tag{9.1}$$

Theorem 9.1. *For each i-th linearly degenerate characteristic field, $i \in II$, there exists $\phi(x)$ such that:*

(1) $\phi(x) = O(1)|x|^{-\frac{3}{2}}$ *as* $|x| \to \infty$*;*

(2) *the solution* $\boldsymbol{u}(x,t)$, $(x.t) \in \tilde{\Omega}_i$, *tends to the corresponding simple wave* $\boldsymbol{\phi}(x,t)$, (9.1), *as* $t \to \infty$ *and the convergence rate is* $t^{-1/2}$ *in* $L_1(x)$.

Proof. In the region $\tilde{\Omega}_i$, the amount of j-waves, $j \neq i$, is of the order of $Q_d(t) + Q_s(t)$, which decays at the rate of $(TV)^3 t^{-3/2}$, (7.2). This and (7.8) imply that

$$\boldsymbol{u}(x,t) \in \boldsymbol{R}_i(\boldsymbol{u}_0) + O(1)(TV)^3 t^{-\frac{3}{2}},\ \lambda_i(\boldsymbol{u})(x,t) = \lambda_i(\boldsymbol{u}_0) + O(1)(TV)^3 t^{-\frac{3}{2}}, \quad \text{for } (x,t) \in \tilde{\Omega}_i \text{ and as } t \to \infty. \tag{9.2}$$

The i-waves in $\tilde{\Omega}_i$ do not decay because of linear degeneracy. The i-waves do not interact among themselves, and change in time of the order of $Q_d(t) + Q_s(t)$, and so the change in time is of the rate $t^{-3/2}$. Thus the solution in $\tilde{\Omega}_i$ tends to a limiting function $\tilde{\boldsymbol{u}}(x,t)$ satisfying

$$\boldsymbol{u}(x,t) - \tilde{\boldsymbol{u}}(x,t) = O(1)t^{-\frac{3}{2}}, \text{ for } (x,t) \in \tilde{\Omega}_i.$$

This implies that

$$\int_{\tilde{\lambda}_{i-1}t}^{\tilde{\lambda}_i t} |\boldsymbol{u}(x,t) - \tilde{\boldsymbol{u}}|(x,t)|dx = O(1)t \cdot (1)t^{-\frac{3}{2}} = O(1)t^{-\frac{1}{2}}.$$

This proves the second statement of (2).

By (9.2), the limiting function $\tilde{\boldsymbol{u}}(x,t)$ satisfies $\tilde{\boldsymbol{u}}(x,t) \in \boldsymbol{R}_i(\boldsymbol{u}_0)$ and $\lambda_i(\tilde{\boldsymbol{u}})(x,t) = \lambda_i(\boldsymbol{u}_0)$. In other words, the limiting function $\tilde{\boldsymbol{u}}(x,t)$ is an i-th simple wave solution of the conservation laws, (2.9). Therefore it is of the form of (9.1) for some stationary wave $\phi(x)$.

From (7.8), the $\boldsymbol{u}(x,t) = \boldsymbol{u}_0 + O(1)t^{-3/2}$ for (x,t) on the edges $x = \tilde{\lambda}_{i-1}t$, $x = \tilde{\lambda}_i t$ of the region $\tilde{\Omega}_i$. By varying $x - \lambda_i(\boldsymbol{u}_0 t > 0$, and with (x,t) on the right edge of $\tilde{\Omega}_i$, we have $x - \lambda_i(\boldsymbol{u}_0)t$ is of the same order as t. Therefore $\boldsymbol{u}(x,t) - \boldsymbol{u}_0$ decays at the rate $t^{-3/2}$. In other words,

$$\boldsymbol{u}(x,t) - \boldsymbol{u}_0 = O(1)t^{-\frac{3}{2}} = O(1)(x - \lambda_i(\boldsymbol{u}_0 t)^{-\frac{3}{2}},$$

and for the limiting function

$$\tilde{\boldsymbol{u}}(x,t) - \boldsymbol{u}_0 = O(1)(x - \lambda_i(\boldsymbol{u}_0 t)^{-\frac{3}{2}}.$$

Similar estimate holds for $x < \lambda_i(\boldsymbol{u}_0)t$. This implies the tail behavior of $\phi(x)$ in (1). □

The main theorem, Theorem 1.1, follows from Theorem 8.1 and Theorem 9.1.

References

1. DiPerna, R. J., Decay and asymptotic behavior of solutions to nonlinear hyperbolic systems of conservation laws, *Indiana Univ. Math. J.*, **24** (1974/75), no.11, 1047-1071.

2. Duhlond, J. W. M., E. R. Cohen, W. K. H. Panofsky and E. Deeds, A determination of the wave forms and laws of propagation and dissipation of ballistic shock waves, *The Journal of the Acoustical Society of America*, **18** (1946), no.1, 97-118.

3. Friedrichs, K. O., Formation and decay of shock waves, *Comm. Appl. Math.*, **1** (1948), 211-245.

4. Glimm, J., Solutions in the large for nonlinear hyperbolic systems of equations, *Comm. Pure Appl. Math.*, **18** (1965), 697-715.

5. Glimm, J. and Lax, P. D., Decay of solutions of systems of nonlinear hyperbolic conservation laws, *Mem. Amer. Math. Soc.*, No. 101 (1970), xvii+112 pp.

6. Hopf, E., The partial differential equation $u_t + uu_x = \mu u_{xx}$, *Comm. Pure Appl. Math.*, **3** (1950), 201-230.

7. Lax, P. D., Hyperbolic systems of conservation laws. II, *Comm. Pure Appl. Math.*, **10** (1957), 537-566.

8. Liu, T.-P., The deterministic version of the Glimm scheme, *Comm. Math. Phys.*, **57** (1977), no.2, 135-148.

9. Liu, T.-P., Decay to N-waves of solutions of general systems of nonlinear hyperbolic conservation laws, *Comm. Pure Appl. Math.*, **30** (1977), no.5, 586-611.

10. Liu, T.-P., Development of singularities in the nonlinear waves for quasilinear hyperbolic partial differential equations, *J. Diff. Equa.*, **33** (1979), no.1, 92-111.

11. Liu, T.-P., Admissible solutions of hyperbolic conservation laws, *Mem. Amer. Math. Soc.*, **30** (1981), no.240, iv+78 pp.

12. Liu, T.-P., Pointwise convergence to N-waves for solutions of hyperbolic conservation laws, *Bull. Inst. Math. Acad. Sinica* **15** (1987), no.1, 1-17.